Optik - International Journal for Light and Electron Optics 199 (2019) 163328

Contents lists available at ScienceDirect

Optik

journal homepage: www.elsevier.com/locate/ijleo

Original research article

Retinal blood vessel segmentation from diabetic retinopathy images using tandem PCNN model and deep learning based SVM

T. Jemima Jebaseeli[a,*], C. Anand Deva Durai[b], J. Dinesh Peter[a]

[a] Department of Computer Science and Engineering, Karunya Institute of Technology and Sciences, Coimbatore 641114, Tamilnadu, India
[b] Department of Computer Science and Engineering, King Khalid University, Abha 61421, Saudi Arabia

ARTICLE INFO

Keywords:
Image segmentation
Blood vessel
Diabetic retinopathy
Neural network
Support vector machine
Fundus image
Feature extraction
Deep learning

ABSTRACT

Diabetic Retinopathy (DR) occurs due to Type-II diabetes. It causes damages to the retinal blood vessels and reason for visual impairment. The predicted center is around the probability of variation in the estimation of retinal veins, and the crisp enrolls vessel development inside the retina. To witness the changes segmentation of retinal blood vessels has to be made. A framework to upgrade the quality of the segmentation results over morbid retinal images is proposed. This framework utilizes Contrast Limited Adaptive Histogram Equalization (CLAHE) for eliminating the background from the source image and enhances the foreground blood vessel pixels, Tandem Pulse Coupled Neural Network (TPCNN) model is endorsed for automatic feature vectors generation, and Deep Learning Based Support Vector Machine (DLBSVM) is proposed for classification and extraction of blood vessels. The DLBSVM parameters are fine-tuned via Firefly algorithm. The STARE, DRIVE, HRF, REVIEW, and DRIONS fundus image datasets are deliberated to assess the recommended techniques. The results render that the proposed technologies improve the segmentation with 80.61% Sensitivity, 99.54% Specificity, and 99.49% Accuracy.

1. Introduction

The retina is a reason for vision; it observes the light and transforms as brain signals to produce the vision. Diabetic Retinopathy (DR) made the outer retinal layer thick. The outer retinal layer is damaged and settles dots and spots around the retina. The lipids and proteins inside the retinal layers are developed as a tiny blot of exudates, microaneurysms, and cotton wool spots [1]. At the advanced stage, the Proliferative Diabetic Retinopathy (PDR) leads to the tractional detachment of retina [2,3]. There are various segmentation procedures recommended by various researchers. But, these methods work only on fundus images without pathological effects [4]; till there are difficulties in segmenting the vascular vessel tree map without any discontinuities.

2. Reviews of related studies

Retinal vessel segmentation is an imperative instrument for revealing the deviations that happen in veins and it provides data around the territory of vessels. The precise segmentation of retinal blood vessel is clinically significant [5]. The screening programs have been launched in many countries. The computerized system considerably eases the load of experts. Ana Salazar Gonzalez et al. [6], employed a graph cut technique. The prior learning process is incorporated to obtain the optimal segmentation. But, the methods are sensitive to noise thus, training datasets would need further improvement. Shahab Aslani et al. [7], adopted a hybrid feature

* Corresponding author.
E-mail address: jemima_jeba@karunya.edu (T.J. Jebaseeli).

https://doi.org/10.1016/j.ijleo.2019.163328
Received 4 March 2018; Received in revised form 17 October 2018; Accepted 29 August 2019

vector. Here, 13 Gabor features are used. If these features are reduced, this may result in detrition of accuracy. George Azzopardi et al. [8] designed a BCOSFIRE filter. Its parameters influence the performance of the filter. Also, there are misclassifications in the reproduced width of the minor vessel. This tends to increase the false positives computations. S. Wilfred Franklin et al. [9] have proposed the Multilayer Perceptron Neural Network (MPNN) to segment the retinal vessels. Here, the weight of the feed forward network is changed by the backpropagation algorithm. Since it is a kind of pixel processing based approach, it has a less amount of accuracy of 95.03%. R. Geetha Ramani et al. [10] introduced the Principle Component Analysis (PCA) method for feature vector generation. At the final stage, mathematical morphological operation [11] and Connected Component Analysis (CCA) is performed. The classification of vessel cluster decreases the sensitivity measure in some cases. M.R.K. Mookiah et al. [12] have proposed the system with 13 substantial features for the Probabilistic Neural Network (PNN) and SVM [13,14]. The algorithm depends on training inputs. This is not suitable for real-time clinical images. Shuangling Wang et al. [15] demonstrated two superior classifiers: CNN [16] is used as feature extractor, and ensemble RF is the trainable classifier. The execution performance of the learning algorithms to a significant degree relies upon the training data [17]. In 2006, Geoff Hinton initially proposed the idea of Deep Learning [18,19]. For instance, Multi-layer Kernel Machines (MKM) [20,21], utilizes the arc-cosine kernel; however, the kernel determination is having a testing issue, which incredibly influences the nature of data representation. The D-SVM [22] is having a dispute to choose the parametric-type such as kernel function, SVMs, and feature's weights are yet unanswered. Moreover, Multilayer Support Vector Machine (MLSVM) [23,24], is trained using gradient-based learning on a min-max plan for optimization. The structure of MLSVM is like a neural network but differs from the deep learning structure. As an outcome, while experiencing numerous parameters of every layer, this strategy is inclined to fall into a local optimum.

2.1. Challenges

The blood vessel segmentation methods [25–27], prevalently utilizes vector geometry, statistical data, image filters, and machine learning techniques to generate the low-level feature vectors to detect the vessel. These methods depend on the utilization of high-quality features or heuristic presumptions to solve the issue. These methods do not use the generalized learning pattern to generate the feature vectors. Hence, it is vulnerable to subjectivity and its strategic nature causes shortcomings. The primary challenge is to design an end-to-end framework which learns from the data with no space learning based heuristic data to recognize both coarse and fine vascular structures. There are several approaches suggested for enhancing PCNN parameters to attain virtuous outcomes. There are no methods to spontaneously determine all the parameters of PCNN to achieve the clear-cut image segmentation [28,29]. While considering the earlier approaches, several algorithms are useful to extort the features from unfussy images and receptive to noise. Also, many algorithms which are incompetent in recognizing the blood vessels from pathological depigmented images.

2.2. Motivations

The unconstrained retinal map is used for the macular weakening treatment. Regardless of a substantial number of inquiries on the extraction of retinal veins, there is a requirement for exact retinal blood vessel extraction framework.

i There are a few impediments that need change, including deceitful vessel extraction which is caused due to low segmentation between the retinal vessels and the background. In like way, the impairment of the blood vessel tree whose topological construction is complex.
ii There is a couple of disenchantment that must be redesigned among the retinal veins and the non-vessel image.
iii The organize network misfortune amidst retinal vessels makes a complex topological structure.
iv In some method, it is inadequate to demonstrate the whole segmentation result if there ought to emerge an event of veins that obscure a long way from the mid to its broadened heading.
v Losing one branch point may prompt a lacking vein system and raises the error. Grounded on this motivation, the proposed TPCNN model is competently deciding the paramount alternative of segments similar to the intended object. Subsequently, it is proficient enough to observe the little veins without any discontinuities.

2.3. Novelty of the proposed techniques

The Tandem PCNN (TPCNN) model extract the blood vessels from the obsessive fundus images and discloses all tiny vessels at their cross boundaries which are suppressed by depigmentation. Deep Learning Based SVM (DLBSVM) improves the classification accuracy in categorizing the vessel pixels from non-vessel pixels. Compared with the conventional methods the proposed methods have the following novelties:

i The scheming of pulse threshold to fire the neuron is computed dynamically.
ii The linking weight redefines the strength of the active neuron.
iii The proposed TPCNN model extracts the blood vessels within four iterations.
iv The cross-channel linking of TPCNN model enables the visibility of vessels at the crossover points.
v Classification and extraction of retinal blood vessels via DLBSVM help the network to attain better data expression to increase the final classification result.
vi Firefly algorithm optimizes the parameters of TPCNN.

Table 1
Fundus Image Databases.

Database	No. of Images	Image size (pixels)
DRIVE	40	584 × 584
STARE	20	700 × 605
REVIEW	16	1360 × 1024
HRF	15	3504 × 2336
DRIONS	110	600 × 400

3. Materials

The fundus images chosen for validation of the proposed approaches are taken from the public datasets such as STARE, DRIVE, HRF, REVIEW, and DRIONS databases [30]. Table 1 describes the number of fundus images taken for the proposed model's experimentation.

The following are the test set and training set images available in the public databases used by various researchers for their experimental setup.

i DRIVE database has 20 test images and 20 training images.
ii STARE database contains 20 images with two sets of manual segmentation provided by two experts. Here, there is no division into training and testing images.
iii REVIEW database encompasses 16 test images.
iv HRF database comprises 15 test images.
v DRIONS database encloses 50 test images and 60 training images.

We have used all the above 201 fundus images to assess the performance of the proposed techniques.

4. Methods

The architecture of the proposed segmentation method is shown in Fig. 2. The blood vessels are extracted by the subsequent ways. At first, the image enhancement and noise removal are done through CLAHE. Then, the feature vectors are produced by Tandem PCNN model. The retinal blood vessels are classified using DLBSVM and segmented using Tandem PCNN's feature element vectors. Firefly algorithm generates values to optimize the parameters of DLBSVM.

4.1. Preprocessing of fundus images

The false photographic artifacts and illumination inconsistencies in the fundus image are preprocessed. The intensity of the green channel has more vessel pixels compared to its background [1,13]. Therefore the green channel is considered and CLAHE preprocesses it. The CLAHE picks the clipping value of the histogram and computes the local histogram amplification of the image. The tile estimate is fixed spontaneously dependent on the vascular geometry of the retinal image. The preprocessed fundus image is shown in Fig. 1.

4.2. Blood vessel segmentation - Tandem PCNN (TPCNN) model

The simple PCNN model is inadequate to complete the segmentation procedure. In multispectral PCNN (m-PCNN), m-channels are fused to create the outcomes. The resultant image provides more details, but it doubles the execution time. Hence, there is a need of

Fig. 1. Preprocessing results of the fundus image (DRIONS).

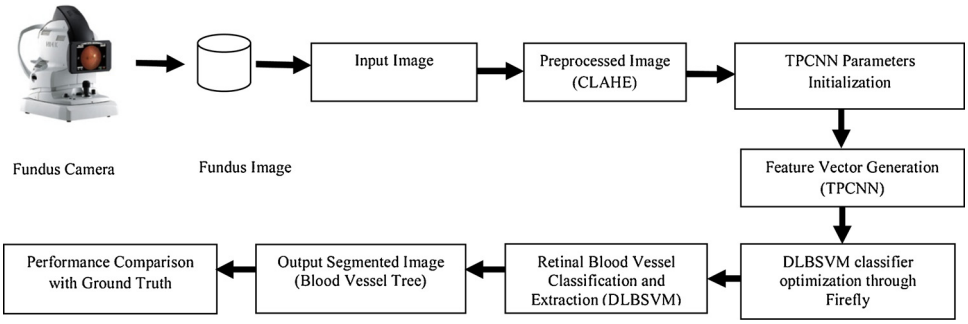

Fig. 2. The recommended frame work for the retinal blood vessel segmentation.

Tandem PCNN model, which fuses the data from two source input images.

Tandem PCNN (TPCNN) model is shown in Fig. 3 which triggers the inter and intra channel linking of the input neurons. The main channel creates an auto wave which stimulates to generate auto waves continuously. Each auto wave generation renowned the edges of the retinal vessels and made it detectable. The cross-channel linking of this model authorizes the visibility of vessels at the crossover points. This model need not bother about the training of the target information. In Tandem PCNN model, there are two input channels such as$f^a$and$f^b$are considered here, instead of feeding input and linking the input field in the basic PCNN model.

$$f^a(n) = s^a + m(y(n-1)) \tag{1}$$

$$f^b(n) = s^b + w(y(n-1)) \tag{2}$$

where$s^a$and $s^b$are input images respectively. m and w are the feeding functions which decide the encompassing neurons.

$$m(.) = y(n-1) \otimes k \tag{3}$$

Where n is the iteration count. $y(n-1)$ is the yield neurons created in the midst of the past cycle. k is the array of convolution core values.

The inertia weight$w$is reduced to the minimum value in the diverse iteration. The adjustment of inertia weight plays an imperative role in improving TPCNN model. In the case of fixed inertia weight, the method traps into local optima. The linear decrease in weight leads to missing optimal point value in the final segmentation. To solve this issue, the inertia weight is redefined as follows,

$$w = w_{\max} - \frac{t(w_{\max} - w_{\min})}{t_{\max}} \tag{4}$$

$$w = \begin{cases} w_{\min} - \dfrac{(w_{\max} - w_{\min}) \times (f^a(n), f^b(n))_t - (f^a(n), f^b(n))_{\min}}{(f^a(n), f^b(n))_{avg}}, & (f^a(n), f^b(n))_t \le (f^a(n), f^b(n))_{avg} \\ w_{\max}, & (f^a(n), f^b(n))_t > (f^a(n), f^b(n))_{avg} \end{cases} \tag{5}$$

where t is the recent iteration, $w_{\max}$ is the maximum weight, and $w_{\min}$ is the minimum weight.

When the fitness estimation of the entire particles had a tendency to join together expands the inertia inactivity weight. At the point when the fitness estimation of all particles distributed, the inertia weight esteem is decreased. Since the inertia weight esteem is logically altered close by the fitness value. The dynamic inertia weight has the accompanying favorable circumstances for those

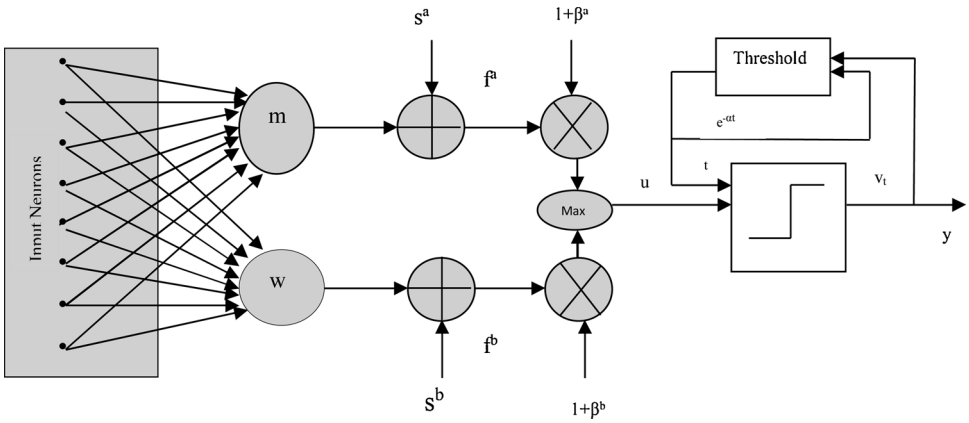

Fig. 3. Tandem Pulse Coupled Neural Network (TPCNN) model.

incredible particles whose fitness esteem are more significant than the normal fitness value; they will normally get the littler weight regard. That suggests they will diminish their speed and be ensured. For those particles whose fitness esteems are more diminutive than the normal fitness esteem, they will normally obtain the more prominent inactivity weight regard. That infers will extend their speed and quickly move closer to the phenomenal particles. The receptive field gets the information and upgrades the enveloping neurons. $u$is the connecting field, where all data are combined to find the state of the neuron to be terminated is processed as,

$$u(n) = \max((1 + \beta^a f^a(n))(1 + \beta^b f^b(n))) + \delta \tag{6}$$

The weighing coefficients off^a and f^b are β^a and β^b. It is expected to decide the quality of the linking neuron. δ is the smooth factor to screen the inner activity of the neuron. To consequently determine the estimation ofβ, the background and the object intensity $[i_1, i_2]$and $[i_3, i_4]$ are analyzed. The smallest linking input of the neuron intensity ($\beta_{\max}$) of $i_1$andi_3 are captured by the firing neuron $i_1 < i_3 < i_2$.

$$\beta_{\min} = \max((i_4/i_3 - 1)/f^a(n), (i_2/i_1 - 1)/f^b(n)) \tag{7}$$

The most extreme linking input of the neuron intensity ($\beta_{\max}$) $i_2$is caught by the firing neuron is,

$$\beta_{\max} = (i_4/i_2 - 1)/\max(f^a(n), f^b(n)) \tag{8}$$

To guarantee all the blood vessels captured by the neighboring neurons are computed using the iterations of Tandem PCNN model is,

$$\beta(n) = i_4(n)/i_2(n-1)/\max(f^a(n), f^b(n)) \tag{9}$$

Where i_4 is the upper bound and i_2 is the lower bound intensity of fired neuron linking input at the TPCNN iteration process. In dissimilarity to the static value ofβ, the conceivable object neurons with spatial proximity is given most priority to fire and creates the reasonable outcome. The pulse generator $y(n)$ generates the output pulse.

$$y(n) = \begin{cases} 1 & u(n) > t(n) \\ 0 & otherwise \end{cases} \tag{10}$$

The dynamic threshold $t(n)$ is expressed by the following equation.

$$t(n) = \begin{cases} e^{-\alpha t} t(n-1) & y(n) = 0 \\ v_t & otherwise \end{cases} \tag{11}$$

$v_t$and $\alpha t$are the normalized offset and time constants. The receptive field gathers the encompassing neurons as a contribution to deciding the feeding and linking field values. The neurons of two channels get the external stimuli from the surrounding neurons. At that point, these channels are weighed and the information is fused according to the weighing coefficients. Then the dynamic neuron will be fired based on the attenuation coefficients. The generated outputs are given to the pulse generator to yield the output pulse.

4.2.1. Algorithm of TPCNN

The algorithm for Tandem PCNN model is as follows.

1. *Input*: s^a, s^b
2. *Let* $u = 0$, $y = 0$, $t = 1$
   Computew and mfrom empirical metrics.
3. *If* $s^a = s^b$*then set* $o \longleftarrow s^a || s^b$
   goto step 7.
4. *Set* $e^{-\alpha t} \longleftarrow [0, 1]$
5. Identify the Surrounding Neurons
   $sn \longleftarrow y[n-1] \otimes k$
   $u(n) \longleftarrow \max((1 + \beta^a f^a(n))(1 + \beta^b f^b(n))) + \delta$
   If $u(n) > t(n)$ *then* $y(n) \longleftarrow u(n) - sn$
   Else $y(n) \longleftarrow 0$
   End
   If $s^a = s^b$ || $\beta^a = \beta^b$*then* $o \longleftarrow s^a || s^b$
   Else $o \longleftarrow y$
   End
   If $y = 0$*then* $t \longleftarrow e^{-\alpha t}$
   Else $t \longleftarrow v_t$
   End
6. Stop when all neurons are fired goto Step 7. Else goto Step 5.
7. Output: $o$is the output of Tandem model PCNN.

4.2.2. Parameter setting

In Tandem PCNN model, the parameters are initialized as follows:

1 Convolution core K = [0.5, 1, 0.5; 0.5, 1, 0.5; 0.5, 1, 0.5]
2 Smooth factor σ = 1.2
3 Time constant $\alpha t = 0.2$
4 Standardized offset parameter $v_t = 220$.

4.3. Retinal blood vessel classification - deep learning based SVM (DLBSVM) model

The training data commencing from the Tandem PCNN model of the form$\{(x_1, y_1), ..., (x_n, y_n)\}$; such that, x_i is the feature vector and $y_i$is the classification label of the image. DLBSVM has the function$G: X \rightarrow Y$, where $X$is the input image space and $Y$is the yield feature space. R is the function with the possible element in the hypothesis space. $x_i \in R^N$, $y_i \in Y = \{1, -1\}$ and $i = 1...n$.

4.3.1. Algorithm of DLBSVM

The algorithm of DLBSVM is stated as follows,

Step 1: Input the training data as follows,

$T = \{I_1(x, y), ..I_n(x_n y_n)\} \in (R^N \times y)^n$

Step 2: Initialize the value of similarity measure between the two points: (σ) trades of the misclassification of training against the decision surface, and (c) value of Radial Basis Function parameters in DLBSVM as follows.

$\sigma = [2^{-8}, ..., 2^8]$ & $c = [2^{-8}, ..., 2^8]$.

Step 3: Iteration loop

for $k = 1...K$

1. *Carryout Tandem PCNN*
2. *Construct new Training data*

$T = \{I(x_1^{k+1}, y_1), ..I(x_n^{k+1}, y_n)\} \in (R^N \times y)^n$

end

Step 4: The final classifier

The classifier depends on the inner product of the test point x and the support vectorx_i^{k+1}. The final solution is to calculate the inner products x_i^{k+1}. $x_i$between all pairs of training points. The DLBSVM classification algorithm has gained in popularity due to its high-performance accuracy.

4.4. Firefly algorithm

The Firefly algorithm optimizes the DLBSVM final classification process. The search technique is established on the social conduct of firefly's communication. The brightness determines the firefly's attractiveness. Hence, the attractiveness between$x$ and$x_i^{k+1}$is proportional to the brightness of a firefly. This is given as an objective function$F(x)$. Hence, $I(x_i) \propto F(x_i)$, where $x_i$is the member of the firefly swarm. $I(x_i)$ is the brightness of the corresponding fireflies. The attractiveness between fireflies x_i and$x_j^{k+1}$are defined by their distance vector$dist_{ij}$.

$$dist_{ij} = \frac{|| x_i - x_j^{k+1} ||}{\sqrt{\sum_{l=1}^{n} (x_{il} - x_{jl}^{k+!})^2}} \tag{12}$$

where $l$is the index of candidate fireflies solutions.

The following equation defines the total sum of initial brightness α_i.

$$\alpha = \alpha_i e^{-\varphi dist_{ij}} \tag{13}$$

ϕ is the light absorption coefficient.

The movement of x_i tox_i^{k+1}during attractiveness is defined as follows,

$$x_{il} = (1 - \alpha) x_{il} + \alpha x_{jl}^{k+1} + u_{il} \tag{14}$$

$$u_{il} = rand_1 - \frac{1}{2} \tag{15}$$

If there is no brighter firefly than the specific fireflies $x_{\max_i}$, then it move arbitrarily according to the following given equation.

$$x_{\max_i} = x_{\max_{il}} + u_{\max_{il}} \tag{16}$$

$$u_{\max_{il}} = rand_2 - \frac{1}{2} \tag{17}$$

$rand_1$ and $rand_2$ are obtained from the$u(0, 1)$uniform distribution.

The Firefly - DLBSVM may converge with the most optimal solution within a limited time when it associates with the feature selection because of its complexity.

Table 2
Performance Measures.

$$Sensitivity = \frac{TP}{TP + FN}$$
$$Specificity = \frac{TN}{TN + FP}$$
$$Accuracy = \frac{TP + TN}{(TP + FN) + (TN + FP)}$$
$$TPR = Sensitivity$$
$$FPR = 1 - Specificity$$

5. Performance analysis

The segmented output image contains the blood vessels. Likewise, the ground truth images contain the blood vessels which are classified manually by the specialists. The vessel pixel values of the ground truth images are compared with the segmented output image to discover the worth of the algorithms in predicting the vessel pixels. The proposed method ensures not to flop in classifying the tiny blood vessels which are created by the diseased particles. The proposed Tandem PCNN model segments the blood vessels within four iterations.

5.1. Metrics – I

The performances of the proposed algorithms are evaluated by the parameters such as True Positive (TP), True Negative (TN), False Positive (FP), and False Negative (FN). TP is a pixel marked as vessel pixel in both ground truth image and in segmented output image; TN is a pixel marked as non-vessel pixel in both ground truth image and in the segmented output image; FP value is a pixel marked as vessel pixel in the segmented output image but as a non-vessel in the ground truth image; and FN is a pixel marked as non-vessel in the segmented output image but as a vessel in the ground truth image.

As shown in Table 2,

i Sensitivity denotes the algorithm's capability to detect the blood vessels correctly.
ii Specificity denotes the algorithm's ability to detect the non-blood vessels correctly.
iii Accuracy is the ratio of the total number of correctly classified pixels to the number of pixels in the image field of view.
iv True Positive Rate (TPR) denotes the fraction of pixels correctly detected as vessel pixels.
v False Positive Rate (FPR) indicates the fraction of pixels incorrectly identified as vessel pixels.

The proposed Tandem PCNN model has enormous performance excellence over the DRIVE database with Sensitivity (80.27%), Specificity (99.80%), and Accuracy (98.98%); STARE database with Sensitivity (80.60%), Specificity (99.70%), and Accuracy (99.70%); REVIEW database with Sensitivity (80.88%), Specificity (98.76%), and Accuracy (99.87%), HRF database with Sensitivity (80.77%), Specificity (99.66%), and Accuracy (98.96%); DRIONS database with Sensitivity (80.54%), Specificity (99.78%), and Accuracy (99.94%) on normal and pathological images as shown in Table 3.

5.2. Metrics – II

The computation time exploration is the significant impediments of the supervised vessel segmentation methods, and the proposed technique is not a special case. The proposed strategy is estimated in a PC with Intel(R) Core(TM) i3-5005U CPU@2.00 GHz processor. As appeared in Table 4, the computational time is less for the proposed method while comparing with other competitive methods. The duration for handling a distinct image is 0.6 s for DRIVE database, and 0.8 s for STARE database. The exhibited effectiveness, robustness, smoothness, and fast execution make the proposed computerized blood vessel segmentation method as a flexible instrument for initial DR detection.

Table 3
Performance outcomes of the proposed method.

Database	Sensitivity%	Specificity%	Accuracy%
DRIVE	80.27	99.80	98.98
STARE	80.60	99.70	99.70
REVIEW	80.88	98.76	99.87
HRF	80.77	99.66	98.96
DRIONS	80.54	99.78	99.94
Average Value	**80.61**	**99.54**	**99.49**

Table 4
Computation time per image.

Methods	DRIVE	STARE
Qiaoliang Li et al. [1]	1.2 min	–
Shahab Aslani et al. [7]	60s	60s
Nagendra Pratap Singh et al. [22]	2.26min	2.4min
A. Colomer et al. [29]	297.07 s	303.64 s
Zhexin Jiang et al. [30]	1.67 s	1.67 s
Chengzhang Zhu et al. [31]	12.16 s	–
Dinesh Pandey et al. [32]	7s	8 s
George Azzopardi et al. [2]	10s	10s
Luiz Carlos Rodrigues et al. [33]	35s	–
Toufique Ahmed Soomro et al. [34]	4.5s	4.5s
Sudeshna Sil Kar et al. [35]	2.25s	2.25s
Proposed Method	**0.6 s**	**0.8 s**

6. Experimental results and discussion

The proposed system is instigated and tested using MATLAB R2010a and verified over STARE, DRIVE, HRF, REVIEW, and DRIONS databases. The segmented vessel map of the fundus images and the relating ground truth image are shown in Figs. 4 and 5. The prevailed vascular tree pattern of input fundus images are checked with the ground truth fundus images and shows more accuracy while comparing with other compatible methods.

Table 5 provides the performance of diverse approaches proposed in the literature in relations of the typical incoherency measurements. Subjectively, the proposed approach segments the maximum vessels without holding any background noise. Quantitatively, this methodology accomplishes highest specificity and accuracy but the lowest sensitivity. The overall performance of this proposed method achieves the average sensitivity of 80.61%, specificity of 99.54%, and accuracy of 99.49%. The depigmentations are expelled from the vessel points proactively by the Tandem PCNN model which made the system to follow every small vessel unseen by this depigmentation. The configuration of BCOSFIRE filter has to be attuned for dissimilar shapes, such as vessels, bifurcations and crossover points at diverse scales [8]. There are inaccuracies in the reconstructed width of the tiny vessel. This offers a reduction in the true positive counts. There is a major struggle in relinking vessel segments that are situated far from the intersections. The classifier has been trained by choosing 300,000 samples randomly from the DRIVE dataset [1]. Additionally, the proposed model automatically generates its feature vectors by DLBSVM through Tandem PCNN model. Tandem PCNN is an unsupervised model, where its parameters must be set ahead of time to create the feature vectors consequently. The PCNN parameters of 2D Otsu [28], takes $\alpha_\theta = 0.2$, $V_L = 1$, $V_\theta = 10\,000$, and $\beta = 0.1$. Compared to 2D Otsu technique, the proposed Tandem PCNN model parameters takes less value; also the iteration count for segmenting the image is less. In the proposed model, the Tandem PCNN parameter contains less parameter, and the template will be generated only one time, but it is suitable for all images. Based on the experimentation, these parameters are optimally tuned. Tandem PCNN model is improved than CNN, which is confirmed in the proposed method by combining the virtues of feature learning and traditional classifier. In SVM, there are opportunities to recognize the false vessel pixels; while, DLSVM significantly identifying the minute vessel pixels from its boundary. CNN neglects to find some tiny vessels around the optic disc. The accuracy of Random Forest is depended upon every classifier and their correlations. Each classifier has less value of correspondences. This is suitable for classification and deterioration on images with incredible noises [15]. Due to the disparity in the image intensity between vessel and background, the optimum blood vessels are sometimes neglected because of the nonappearance of the edges [13].

There are various web-based retinal image segmentation tools such as ROPTOOL, VAMPIRE, SIVA, and LIVE VESSEL [31] accessible for Diabetic Retinopathy diagnosis. The android systems [31,33], developed for small datasets could analyze the information within the restricted area nearby the optic disc. Additionally, the processing time is more for a single image. Clinically this solution is unfeasible. Consequently, the proposed Tandem PCNN model with DLBSVM conquers the impediments happened in web-based and Android applications.

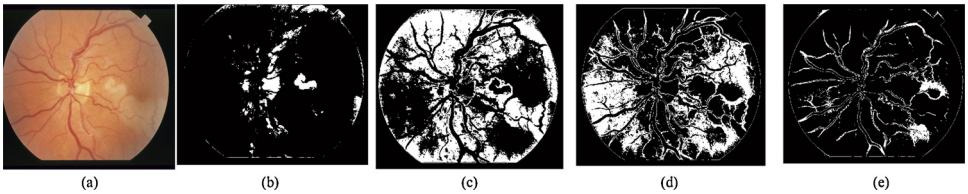

Fig. 4. Segmentation results of STARE Dataset (a) Input image, (b)–(e) Segmentation at four different iterations: i = 0, i = 1, i = 2, i = 3, (e) Final Segmentation image.

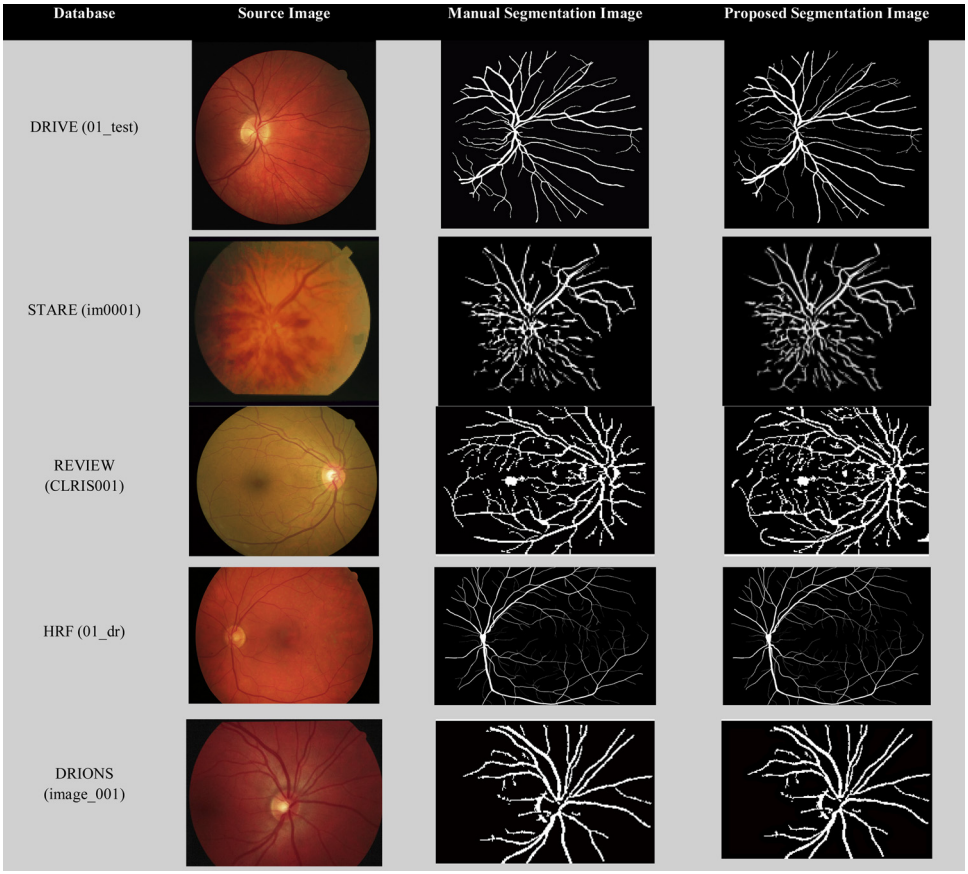

Fig. 5. The comparison of the proposed technique with manual segmentation.

Table 5
Performance comparison with competitive methods for retinal blood vessel segmentation.

Type	Author	Year	Method	Sensitivity %	Specificity %	Accuracy %
Supervised	Qiaoliang Li et al. [16]	2016	Cross-Modality Learning Approach	75.69	98.16	95.27
	Argyrios Christodoulidis et al. [2]	2016	Multi-Scale Tensor Voting Approach	85.06	95.82	94.79
	Shahab Aslani et al. [34]	2016	Multi-scale Gabor wavelet & B-COSFIRE Filters	75.45	98.01	95.13
	Villalobos-Castaldi et al. [35]	2010	Gray Level Co-occurrence Matrix (GLCM)	96.48	94.80	97.59
	Roberto Vega et al. [36]	2015	Lattice Neural Networks with Dendritic Processing	74.44	96.00	94.12
	Elaheh Imani et al. [11]	2015	Morphological Component Analysis	75.24	97.53	95.23
Unsupervised	George Azzopardi et al. [8]	2014	B-COSFIRE Filters	76.55	97.04	96.14
	Miguel A. Palomera-Perez et al. [37]	2010	Parallel Multiscale Feature Extraction and Region Growing	–	–	92.00
	R. GeethaRamani et al. [10]	2016	Gabor Filter & Principal Component Analysis	70.79	97.78	95.36
	Behdad Dashtbozorg et al. [38]	2014	Graph-Based A/V Classification	90.00	84.00	87.40
	Lei Zhang et al. [39]	2015	Multi-Scale Textons	78.12	96.68	95.04
	Nagendra Pratap Singh et al. [40]	2016	Gumbel Probability Distribution Based Matched Filter	75.94	–	95.22
	Rashmi Panda et al. [14]	2016	Binary Hausdorff Symmetry Seeded Region Growing	73.37	97.52	95.39
	Proposed TPCNN, DLBSVM and Firefly Model		**Average value**	**80.61**	**99.54**	**99.49**

7. Conclusions

The proposed techniques are appropriate for the prescreening scheme of Diabetic Retinopathy. The Contrast Limited Adaptive Histogram Equalization improves the contrast of the image and removes the noise from the images captured at different illuminations. Tandem Pulse Coupled Neural Network model fuses two source images and generates the feature vectors to segment the retinal

vasculature. The produced feature vectors are utilized by Deep Learning Based Support Vector Machine technique to classify the vessels from non-vessels. DLBSVM uses numerous layers and decreases the errors in misclassifying the vessel pixels from non-vessel pixels. TPCNN model calibrates its parameters, so that error is limited. Firefly algorithm optimizes the parameters in classifying the vessel pixels. The segmented retinal vessels are compared with the ground truth images and the performance of the algorithm is analyzed. The proposed method facilitates the ophthalmologists in the diagnosis of Diabetic Retinopathy by considering the segmented retinal blood vessels structure. This work can be extended by quantifying the tortuosity of the vessel to distinguish the disease.

References

[1] M. Islamuddin Ahmed, M. Ashraful Amin, High speed detection of optical disc in retinal fundus image, SIViP 9 (2015) 77–85.
[2] A. Christodoulidis, T. Hurtut, H.B. Tahar, F. Cheriet, A multi-scale tensor voting approach for small retinal vessel segmentation in high resolution fundus images, Comput. Med. Imaging Graph. 52 (September) (2016) 28–43.
[3] S.H. Mohammad Alipour, H. Rabbani, M. Akhlaghi, A new combined method based on curvelet transform and morphological operators for automatic detection of foveal avascular zone, SIViP 8 (2014) 205–222.
[4] S.R. Nirmala, S. Dandapat, P.K. Bora, Wavelet weighted distortion measure for retinal images, SIViP 7 (2013) 1005–1014.
[5] Y. Zhao, X. Wang, X. Wang, F.Y. Shih, Retinal vessels segmentation based on level set and region growing, Pattern Recognit. 47 (2014) 2437–2446.
[6] A. Salazar-Gonzalez, D. Kaba, Y. Li, Xiaohui, Segmentation of the blood vessels and optic disk in retinal images, IEEE J. Biomed. Health Inform. 18 (November (6)) (2014).
[7] S. Aslani, H. Sarnel, A new supervised retinal vessel segmentation method based on robust hybrid features, Biomed. Signal Process. Control 30 (September) (2016) 1–12.
[8] G. Azzopardi, N. Strisciuglio, M. Vento, N. Petkov, Trainable COSFIRE filters for vessel delineation with application to retinal images, Med. Image Anal. 19 (2015) 46–57.
[9] S. Wilfred Franklin, S. Edward Rajan, Computerized screening of diabetic retinopathy employing blood vessel segmentation in retinal images, Biocybern. Biomed. Eng. 34 (2014) 117–124.
[10] R. GeethaRamani, L. Balasubramanian, Retinal blood vessel segmentation employing image processing and data mining techniques for computerized retinal image analysis, Biocybern. Biomed. Eng. 36 (1) (2016) 102–118.
[11] E. Imani, M. Javidi, H.-R. Pourreza, Improvement of retinal blood vessel detection using morphological component analysis, Comput. Methods Programs Biomed. 118 (2015) 263–279.
[12] M.R.K. Mookiah, U. Rajendra Acharya, R.J. Martis, C.K.C.C.M. Lim, E.Y.K. Ng, A. Laude, Evolutionary algorithm based classifier parameter tuning for automatic diabetic retinopathy grading: a hybrid feature extraction approach, Knowledge Based Syst. 39 (2013) 9–22.
[13] R. Vega, G. Sanchez-Ante, L.E. Falcon-Morales, H. Sossa, E. Guevara, Retinal vessel extraction using Lattice Neural Networks with dendritic processing, Comput. Biol. Med. 58 (2015) 20–30.
[14] R. Panda, N.B. Puhan, G. Panda, New Binary Hausdorff Symmetry measure based seeded region growing for retinal vessel segmentation, Biocybern. Biomed. Eng. 3 (6) (2016) 119–129.
[15] S. Wang, ilong Yin, G. Cao, B. Wei, Y. Zheng, G. Yang, Hierarchical retinal blood vessel segmentation based on feature and ensemble learning, Neurocomputing 149 (2015) 708–717.
[16] Q. Li, I.E.E.E. Member, B. Feng, L.P. Xie, P. Liang, H. Zhang, T. Wang, A cross-modality learning approach for vessel segmentation in retinal images, IEEE Trans. Med. Imaging 35 (January (1)) (2016).
[17] Y. Bengio, A. Courville, P. Vincent, Representation learning: a review and new perspectives, IEEE Trans. Pattern Anal. Mach. Intell. 35 (8) (2013) 1798–182.
[18] G.E. Hinton, S. Osindero, Y.-W. Teh, A fast learning algorithm for deep belief nets, Neural Comput. 18 (7) (2006) 1527–1554.
[19] G.E. Hinton, R.R. Salakhutdinov, Reducing the dimensionality of data with neural networks, Science 313 (5786) (2006) 504–507.
[20] Y. Cho, L.K. Saul, Kernel methods for deep learning, NIPS (2009) 342–350 9.
[21] Y. Cho, L.-K. Saul, Large-margin classification in infinite neural networks, Neural Comput. 22 (10) (2010) 2678–269.
[22] A. Abdullah, R.C. Veltkamp, M.A. Wiering, An ensemble of deep support vector machines for image categorization, SOCPAR'09 (2009) 301–306.
[23] M. Wiering, M. Schutten, A. Millea, A. Meijster, L. Schomaker, Deep support vector machines for regression problems, Proceedings of the International Workshop on Advances in Regularization, Optimization, Kernel Methods, and Support Vector Machines: Theory and Applications (2013).
[24] M. Wiering, M. Van der Ree, M. Embrechts, M. Stollenga, A. Meijster, A. Nolte, L. Schomaker, The neural support vector machine, Proceedings of the 25th Benelux Artificial Intelligence Conference (BNAIC) (2013).
[25] M.D. Abramoff, M.K. Garvin, M. Sonka, Retinal imaging and image analysis, IEEE Rev. Biomed. Eng. 3 (2010) 169–208.
[26] N. Patton, T.M. Aslam, T. MacGillivray, I.J. Deary, B. Dhillon, R.H. Eikelboom, K. Yogesan, I.J. Constable, Retinal image analysis: concepts, applications and potential, Progress Retinal Eye Res. 25 (1) (2006) 99–127.
[27] J. Staal, M.D. Abramoff, M. Niemeijer, M.A. Viergever, B. van Ginneken, Ridge-based vessel segmentation in color images of the retina, IEEE Trans. Med. Imaging 23 (April (4)) (2004) 501–509.
[28] C. Yao, H. Chen, Automated retinal blood vessels segmentation based on simplified PCNN and fast 2D-Otsu algorithm, J. Cent. South Univ. Technol. 16 (2009) 0640–0646.
[29] T. Jemima Jebaseeli, D. Sujitha Juliet, C. Anand Devaduri, Segmentation of retinal blood vessels using pulse coupled neural network to delineate diabetic retinopathy, Digital Connectivity – Social Impact Volume 679 of the Series Communications in Computer and Information Science, Springer, 23 November, 2016, pp. 268–285.
[30] DRIVE: Digital Retinal Image for Vessel Extraction, http://www.isi.uu.nl/Research/Databases/DRIVE, STARE: http://cecas.clemson.edu/~ahoover/stare/, REVIEW:http://reviewdb.lincoln.ac.uk/Image%20Datasets/Review.aspx, HRF: https://www5.cs.fau.de/research/data/fundus-images/, DRIONS: http://www.ia.uned.es/~ejcarmona/DRIONS-DB.html.
[31] M.M. Fraz, S.A. Barman, P. Remagnino, A. Hoppe, A. Basit, B.U. yyanonvara, A.R. Rudnicka, C.G. Owen, An approach to localize the retinal blood vessels using bit planes and centerline detection, Comput. Methods Programs Biomed. 108 (2012) 600–616.
[32] A. Bourouis, M. Feham, M.A. Hossain, L. Zhang, An intelligent mobile based decision support system for retinal disease diagnosis, Decis. Support Syst. 59 (2014) 341–350.
[33] P. Prasanna, S. Jain, N. Bhagatt, A. Madabhushi, Decision support system for detection of diabetic retinopathy using smartphones, 7th International Conference on Pervasive Computing Technologies for Healthcare and Workshops (2013).
[34] S. Aslani, H. Sarnel, A new supervised retinal vessel segmentation method based on robust hybrid features, Biomed. Signal Process. Control 30 (September) (2016) 1–12.
[35] F.M. Villalobos-Castaldi, E.M. Felipe-Riverón, L.P. Sánchez-Fernández, J. Vis. 13 (2010) 263.
[36] R. Vega, G. Sanchez-Ante, L.E. Falcon-Morales, H. Sossa, E. Guevara, Retinal vessel extraction using Lattice Neural Networks with dendritic processing, Comput. Biol. Med. 58 (2015) 20–30.
[37] M.A. Palomera-Perez, M. Elena Martinez-Perez, H. Benıtez-Perez, Jorge Luis Ortega-Arjona, parallel multiscale feature extraction and region growing: application in retinal blood vessel detection, IEEE Trans. Inf. Technol. Biomed. 14 (March (2)) (2010).
[38] B. Dashtbozorg, A.M. Mendonça, A. Campilho, An automatic graph-based approach for Artery/Vein classification in retinal images, IEEE Trans. Image Process. 23 (March (3)) (2014).
[39] L. Zhang, M. Fisher, W. Wang, Retinal vessel segmentation using multi-scale textons derived from key points, Comput. Med. Imaging Graph. 45 (2015) 47–56.
[40] N.P. Singh, R. Srivastav, Retinal blood vessels segmentation by using Gumbel probability distribution function based matched filter, Comput. Methods Programs Biomed. 129 (2016) 40–50.